Polym. Bull. (2015) 72:2455–2469
DOI 10.1007/s00289-015-1423-3

ORIGINAL PAPER

Synthesis of peanut shell/polyacrylonitrile copolymer via Cu(0)-mediated RDRP and its adsorption behavior after modification

Liangjiu Bai[1] · Dongju Wang[1] · Hou Chen[1] · Dongxin Li[1] · Yuanyuan Xu[1] · Lili Yu[1] · Wenxiang Wang[1]

Received: 7 January 2015 / Revised: 24 April 2015 / Accepted: 29 May 2015 /
Published online: 9 June 2015

Abstract Peanut shell (PNS) was used to prepare a novel adsorbent to achieve resource recovery of the agricultural residue. The hydroxyl groups of peanut shell were turned into $–C(CH_3)_2–Br$ pendant groups to initiate polymerization of acrylonitrile. Graft copolymer peanut shell/polyacrylonitrile (PNS-*g*-PAN) was modified by hydroxylamine hydrochloride to transform the cyano groups into amidoxime (AO) groups. The modified copolymer of AO-PNS-*g*-PAN was used as adsorbent. The maximum adsorption capacity for Hg(II) was 4.45 mmol g^{-1}. The adsorption process fitted well the Freundlich isotherm model and followed pseudo-second-order model. The modified copolymer demonstrated its potential as an efficient adsorbent to solve the problem of Hg(II) contamination.

Graphical abstract The peanut shell (PNS) macroinitiator was obtained by acylation of hydroxyl groups on the cellulose backbone of the peanut shell and initiated by Cu(0)-mediated RDRP of acrylonitrile. PNS-*g*-PAN was modified by $NH_2OH{\cdot}HCl$ and used to remove heavy metal ions. The maximum adsorption capacity of Hg(II) was 4.45 mmol g^{-1}.

✉ Liangjiu Bai
bailiangjiu@163.com

✉ Hou Chen
lduchenhou@126.com

[1] School of Chemistry and Materials Science, Ludong University, Yantai 264025, China

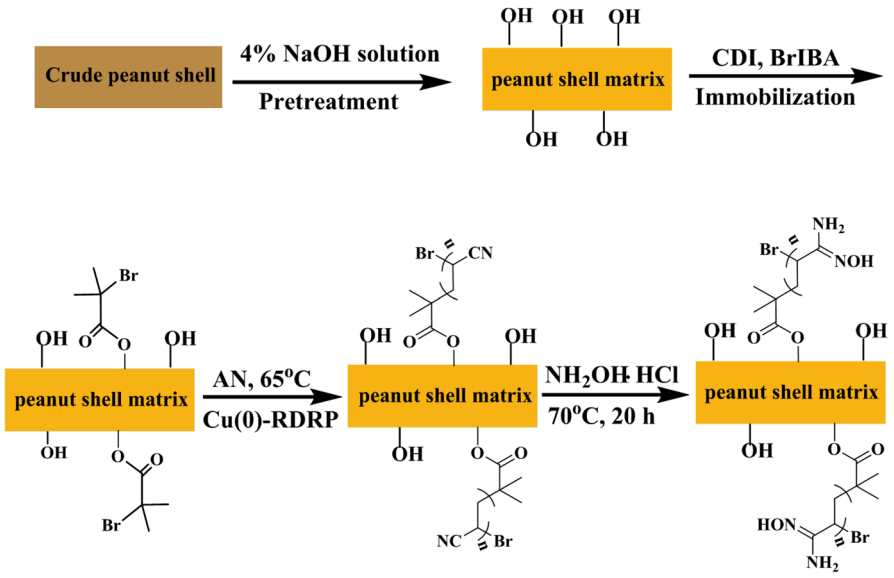

Keywords RDRP · Polyacrylonitrile · Cu(0)-mediated RDRP · Peanut shell · Hg(II)

Introduction

Increasing industrial activities such as oil refining and battery manufacturing industries resulted in the heavy metal ions contamination in surface and ground water [1, 2]. The anthropogenic contamination of Hg(II) ions not only endangered the human health but also caused environmental problems [3, 4]. Adsorption is one of the most effective and potential methods owing to its strong affinity and high loading capacity for heavy metal ions. A low-cost adsorbent such as agricultural residue has received increasing attention due to its advantages of inherent adsorption property, simple technique, and little processing in comparison with activated carbon. According to Babarinde et al. [5], maize leaf was employed as an efficient adsorbent for removal of lead from aqueous solutions. Sago was used as an adsorbent to adsorb lead and copper by Quek et al. [6]. Synthetic polymer was also used as the adsorbent for heavy metal ions owing to its relative high selectivity [7, 8]. Niu et al. reported that the silica gel supported hyperbranched polyamidoamine dendrimers (SiO_2-G0–SiO_2-G4.0) exhibited great potential to remove Pb(II) from aqueous solution [9]. Recent interest in combining agricultural residue with synthetic polymer to prepare blend and efficient adsorbent has grown significantly. Vijayalakshmi et al. prepared the cellulose acetate and polycarbonate blend ultrafiltration membranes by the phase inversion technique and used the membranes to remove heavy metal ions [10].

The available reversible deactivated radical polymerization (RDRP, or named as "living"/controlled radical polymerization) methods to prepare graft copolymer include nitroxide-mediated polymerization (NMP) [11], reversible addition fragmentation chain transfer (RAFT) [12, 13], atom transfer radical polymerization (ATRP) [14], and Cu(0)-mediated reversible-deactivation radical polymerization [Cu(0)-mediated RDRP, or named as single electron transfer-living radical polymerization] [15]. Comparing with other polymerization methods, Cu(0)-mediated RDRP proved its potential as an alternative for higher polymerization rate and lower extent of recombination of the growing polymer [16–18]. The versatility and controllability of Cu(0)-mediated RDRP provide a series of opportunities to specifically graft from brominated cellulose thereby producing desirable graft copolymer [19].

Peanut shell which contained abundant cellulose was selected as our raw materials owing to its inherent adsorption property to heavy metal ions [20]. Moreover, the adsorption property of peanut shell can be improved by grafting synthetic polymers to its surface through Cu(0)-mediated RDRP. Polyacrylonitrile (PAN) was known as an important precursor to polymer materials due to its unique properties. The cyano groups of PAN can be easily modified to generate amidoxime (AO) groups which can form stable chelating compounds with heavy metal ions.

In this study, our primary objective was to prepare a kind of adsorbent containing both hydroxyl groups and amidoxime groups. Peanut shell was first pretreated by the processes of alkalization and acylation. Brominated peanut shell was employed as initiator in the preparation of PAN via Cu(0)-mediated RDRP. The resulting copolymer peanut shell/polyacrylonitrile (PNS-*g*-PAN) was modified by hydroxylamine hydrochloride ($NH_2OH{\cdot}HCl$) to generate amidoxime (AO) groups. The modified copolymers were used as adsorbents to solve the pollution of Hg(II) in water.

Materials and methods

Materials

Peanut shell was purchased from Yantai Farmers Market. Acrylonitrile (AN) was bought from Fuchen Chemical Reagents (Tianjin, China), which was distilled under normal pressure and stored at −20 °C. Dimethyl sulfoxide (DMSO) 99.5 %, Cu(0) powder (analytical grade), *N*,*N*-dimethylformamide (DMF, analytical grade), *N*,*N*,*N*′,*N*′-tetramethylethylenediamine (TEMED), *N*,*N*′-carbonyldiimidazole (CDI), α-bromoisobutyric acid (α-BrIBA), and imidazole were supplied by Aladdin Chemistry and used without further purification.

Pretreatment of peanut shell (PNS)

PNS was soaked in distilled water for 24 h after removing the impurities. The above PNS was crushed, sifted by 100 mesh's sieve, washed with distilled water, and dried

at 50 °C until constant weight. Then, the peanut shell powder was alkalized by 4 % sodium hydroxide (NaOH) solution at 55 °C for 2 h and then named as PNS matrix.

Immobilization of initiator on the PNS matrix

PNS macroinitiator was prepared by the acylation of hydroxyl groups with α-BrIBA. 4.33 g CDI and 4.45 g α-BrIBA were stirred in 60 mL DMSO at 25 °C for 1 h to form the imidazoyl-activated acid derivative. 1.81 g imidazole was added as additional catalyst and the mixture was heated to 50 °C. The above solution was put into the flask that contained 3.0 g peanut shell powder and 40 mL DMSO. The flask was sealed and reacted at 50 °C for 2 h. The resulting products were precipitated in 2-propanol, filtered and extracted for 24 h with 2-propanol [21, 22].

Preparation of PAN using peanut shell macroinitiator

The amounts of peanut shell macroinitiator (1.0 g), Cu(0) powder (9.7 mg), TEMED (91.1 μL), DMF (10 mL), and AN (10 mL) were added into a 100-mL two-necked flask that was immersed in ice water under stirring. The mixture was bubbled with nitrogen for 20 min to evict oxygen dissolved in solution. Then, the mixture was degassed with three nitrogen-vacuum-nitrogen cycles. Finally, the flask was filled with nitrogen and immersed in an oil bath at 65 °C. After the definite polymerization time, the product was removed and precipitated in methanol/water (v:v = 1:1) solution for 24 h. The precipitate was separated by filtration and dried until a constant weight at 60 °C. The graft copolymer peanut shell/polyacrylonitrile (PNS-*g*-PAN) (2.25 g) was obtained finally.

Modification of PNS-*g*-PAN with $NH_2OH{\cdot}HCl$

2.0 g PNS-*g*-PAN and 2.5 g $NH_2OH{\cdot}HCl$ were stirred in 20 mL methanol for 2 h in the reactor. The solution pH was adjusted to 9.0 using NaOH and the mixture was stirred at 70 °C for 20 h. Modified PNS-*g*-PAN was dried until a constant weight at 60 °C and referred to as the adsorbent AO-PNS-*g*-PAN [23]. The corresponding synthetic routes are illustrated in Fig. 1.

Adsorption characteristics

Effect of pH on adsorption

AO-PNS-*g*-PAN (10 mg) and 20 mL of 0.005 mol L^{-1} Hg(II) solution (pH = 1.0–7.0) were equilibrated in a 100 mL Erlenmeyer flask for 24 h at 25 °C. Then, 4 mL solution was taken out, diluted and detected by atomic absorption spectrometry (AAS). The adsorption capacity of AO-PNS-*g*-PAN was calculated according to the following Eq. (1):

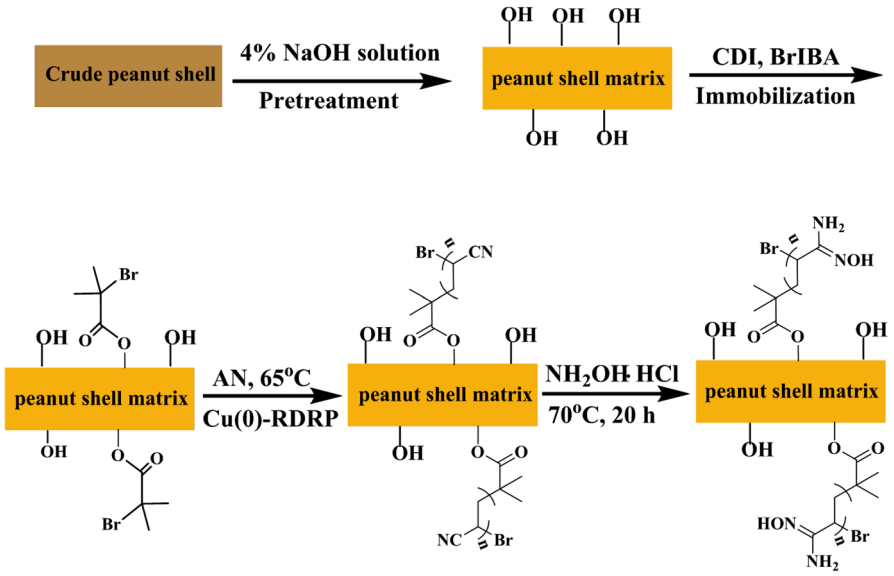

Fig. 1 Scheme for synthesis of adsorbent AO-PNS-*g*-PAN

$$q = \frac{(C_0 - C)V}{W} \tag{1}$$

where q is the adsorption capacity (mmol g^{-1}), C_0 and C are initial and final concentrations of metal ions in solution, W is the weight of adsorbent (mg), and V is the volume (mL).

Adsorption kinetics

Adsorption kinetics were conducted by the following procedures: a series of 100-mL flasks were loaded with 10 mg AO-PNS-*g*-PAN and 20 mL of 0.005 mol L^{-1} Hg(II) solution (pH = 6.0). Then, the flasks were shaken at a definite temperature and taken out at various time intervals. 4 mL solution was extracted from every flask and diluted to 25 mL with distilled water, and the concentration of Hg(II) was determined via AAS.

Adsorption isotherms

Adsorption isotherms were investigated by shaking a series of 100-mL flasks for 24 h, which contained 10 mg AO-PNS-*g*-PAN and 20 mL of different initial metal ion concentrations. The variations of Hg(II) concentration were determined by the AAS.

Characterization

Wide-angle X-Ray diffraction (WAXRD) measurements were performed on a Rigaku DMax-2500 with Cu Ka radiation ($\lambda = 0.1542$ nm). Fourier transform infrared (FTIR) spectroscopy was recorded on Nicolet MAGNAIR550 spectrophotometer, using potassium bromide pellets at a resolution of 4 cm^{-1}. Scanning electron microscopy (SEM) was used to observe the micrographs of products. Atomic adsorption spectrophotometer (932B-model, AAS, GBC, Australia) was equipped with air–acetylene flame and used to determine the concentrations of Hg(II) ions. The conversion of AN (2) and the grafting ratio (the degree of grafting polymerization) (3) [24] were calculated by gravimetry via the following equations:

$$\text{Conversion } (\%) = (m_{\text{PNS-}g\text{-PAN}} - m_{\text{macroinitiator}})/m_{\text{AN}} \times 100\ \% \quad (2)$$

$$\text{Graft ratio } (\%) = (m_{\text{PNS-}g\text{-PAN}} - m_{\text{macroinitiator}})/m_{\text{macroinitiator}} \times 100\ \% \quad (3)$$

where $m_{\text{PNS-}g\text{-PAN}}$, $m_{\text{macroinitiator}}$ and m_{AN} refer to the weights of the copolymer PNS-*g*-PAN, macroinitiator and monomer AN, respectively.

Results and discussion

Peanut shell was used as a substrate to prepare the adsorbent. The primary reaction routes includes: (1) pretreatment of peanut shell, (2) preparation of macroinitiator, (3) synthesis of PNS-*g*-PAN via Cu(0)-mediated RDRP, and (4) modification of PNS-*g*-PAN.

Pretreatment of peanut shell

The alkalization of peanut shell was used to remove some impurities and obtain useful cellulose that could conduct acylation through hydroxyl groups on the hexose units. X-ray diffraction patterns of the crude and alkalized peanut shell samples are presented in Fig. 2. The XRD profile of peanut shell cellulose revealed that the characteristic peak was $2\theta = 23°$. The existence of sharp peak at $2\theta = 23°$ in Fig. 2a indicates that the cellulose molecules of peanut shell are arranged in ordered lattice in which hydroxyl groups are bonded by strong secondary forces. After alkalized by 4 % NaOH solution, the peak of peanut shell had an obvious decrease at the $2\theta = 23°$ as shown in Fig. 2b. The results indicated a decrease in the crystalline nature of peanut shell structure, which was beneficial to the acylation process [25].

Preparation of peanut shell macroinitiator

Peanut shell macroinitiator was prepared by the substitution of hydroxyl groups with other functional groups containing bromine atoms. The cellulose was brominated using α-BrIBA through the immobilization process in Fig. 1. The emergence of carbonyl peak at 1736 cm^{-1} in Fig. 3b demonstrated that the

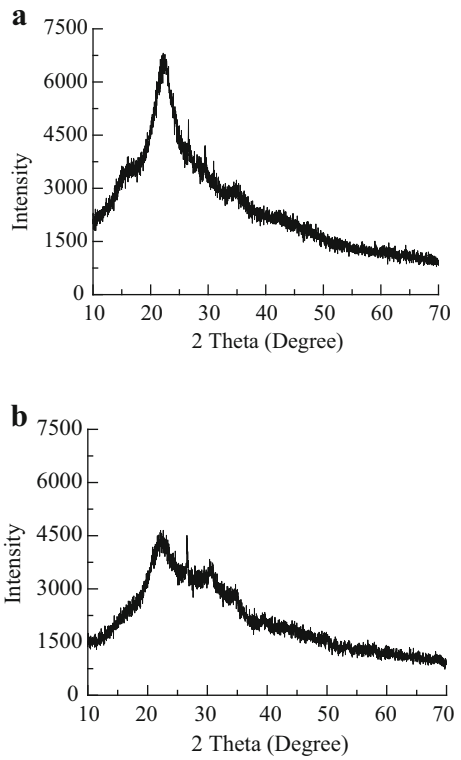

Fig. 2 X-ray diffractograms of untreated and pretreated peanut shell **a** untreated peanut shell, **b** alkalined peanut shell with 4 % NaOH

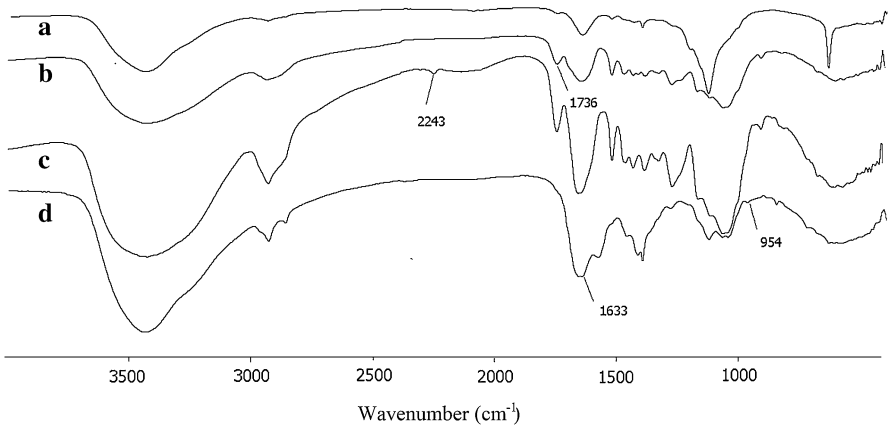

Fig. 3 FTIR spectrum of crude peanut shell powder (*a*), peanut shell macroinitiator (*b*), PNS-*g*-PAN (*c*), and AO-PNS-*g*-PAN (*d*)

immobilization process was conducted successfully comparing to the peak of crude peanut shell in Fig. 3a. The simple and low-energy pretreatment cannot significantly improve the accessibility and reactivity of cellulose, which may result in the low degree of substitution.

Kinetic experiments

The reactions were carried out independently with the same molar ratio of $[AN]_0/[Cu(0)]_0/[TEMED]_0 = 200/0.2/0.8$ through Cu(0)-mediated RDRP. As shown in Fig. 4, the linearity of the plot indicated that the polymerization was approximately first order with respect to the monomer concentration, and the conversion of the monomer increased smoothly with time prolonged. The long induction period might be assumed to the fact that initiating sites were anchored on cellulose chains and large space steric hindrance was existed. The length and hindrance of cellulose chains also influenced the equilibrium rate between the dormant and active growing centers. The monomer conversion and grafting ratio [24] were calculated to be 15.5 and 125.0 % according to Eqs. (2) and (3), respectively. Referring to the low monomer conversion, we attributed to the following reasons. First,the substrate used to prepare macroinitiator (PNS) was peanut shell powder with lower specific surface area comparing to the cellulose nanocrystals and there existed a large number of intermolecular hydrogen-bonding interaction due to the inadequate process. Owing to the large space steric hindrance, only C_6-hydroxyl group has a relatively high reactivity on the glucose units. Meanwhile, from the point of living radical polymerization, the existence of the steric hindrance increased the partial termination of living free radicals which result in losing the initiation function of part of dormant species [26, 27].

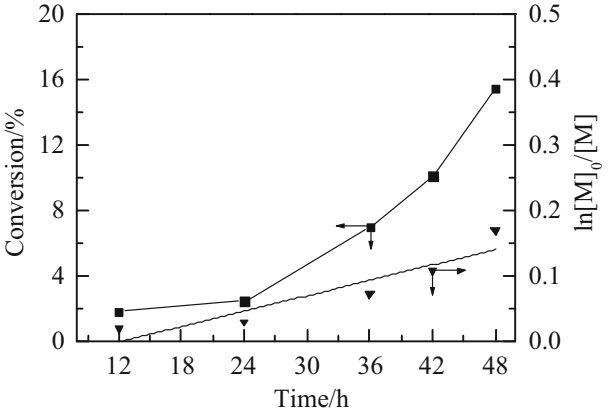

Fig. 4 Kinetic plot for Cu(0)-mediated RDRP of AN at 65 °C in DMF with [AN] = 7.55 M and $[AN]_0:[Cu]_0:[TEMED]_0 = 200:0.2:0.8$, $m_{macroinitiator} = 1.0$ g

Modification of PNS-*g*-PAN with $NH_2OH{\cdot}HCl$

The CN groups of PNS-*g*-PAN were converted to AO groups through reacting with $NH_2OH{\cdot}HCl$. FTIR spectra of PNS-*g*-PAN and AO-PNS-*g*-PAN are shown in the Fig. 3c, d, respectively. The disappearance of CN group spectrum at 2243 cm^{-1} and the emergence of new peaks at 1633 and 954 cm^{-1} which, respectively, corresponded to the stretching vibration of C–N and N–O bonds of AO groups demonstrated the success of the modification. SEM images in Fig. 5 displayed the changes in the morphology of the crude peanut shell (a), peanut shell macroinitiator (b), PNS-*g*-PAN (c), and AO-PNS-*g*-PAN (d). Comparing with the smooth surface of crude peanut shell (a), the surface of peanut shell macroinitiator (b) became rough and uneven due to the swelling effect of NaOH and DMF solution. As the polymerization of AN proceeded, the surface of peanut shell was partly covered with polymer as shown in Fig. 5c. It is more obvious that on the surface of AO-PNS-*g*-PAN (d) appeared the crystal analogs and pore shapes with the completion of the last modification. The existence of porous and loose structure on adsorbent surface is beneficial to adsorption process.

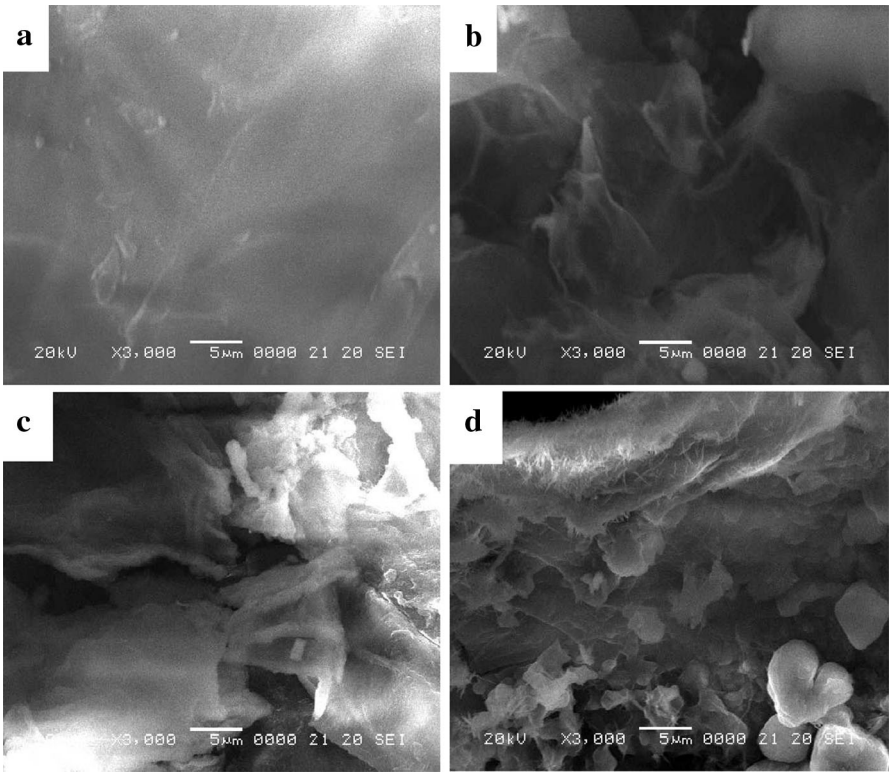

Fig. 5 SEM micrographs of crude peanut shell powder (**a**), peanut shell macroinitiator (**b**), PNS-*g*-PAN (**c**), and AO-PNS-*g*-PAN (**d**)

Adsorption properties

The adsorption capacity of both AO-PNS-*g*-PAN and crude peanut shell under the same condition were determined. The maximum adsorption capacity of AO-PNS-*g*-PAN and alkalized peanut shell for Hg(II) at 45 °C was 4.45 and 0.92 mmol g^{-1}, respectively. In the following part, the effect of pH, adsorption kinetics and adsorption isotherms of AO-PNS-*g*-PAN for Hg(II) were further studied.

Optimization of the adsorption pH

The solution pH is deemed as an indispensable factor that remarkably affects the charge states of the adsorbent surface and the degree of ionization of metal ions in solution. The effect of pH on the adsorption capacity is presented in Fig. 6. It showed that the adsorption capacity of AO-PNS-*g*-PAN for Hg(II) was pH-dependent and the maximum adsorption capacity was obtained at pH = 6.0. At low pH, most of the functional groups on adsorbent surface (such as $–NH_2$ and –OH) are protonated and presented in the positively charged form, which reduce the number of active binding sites [28]. Also, the electrostatic repulsion between Hg(II) and the positively charged functional groups may prevent the adsorption of Hg(II) onto the surface of the adsorbents [29, 30]. Therefore, the adsorption of Hg(II) in acidic solution was unfavorable. As pH increases, most of the protonated $–NH_2$ and –OH groups are gradually deprotonated and more active binding sites available, which would promote the formation of the complex with Hg(II), and hence the adsorption capacity increased [31]. The high adsorption capacity of AO-PNS-*g*-PAN for Hg(II) further demonstrated that the chelating effect of amidoxime groups and loose structure played an important role in the adsorption process.

Adsorption kinetics

Figure 7 depicts the effect of contact time on the adsorption of AO-PNS-*g*-PAN to Hg(II) at 25, 35, 45 °C, respectively. The kinetic curves indicated that the maximum adsorption was obtained at 45 °C. As presented in Fig. 7, the adsorption process

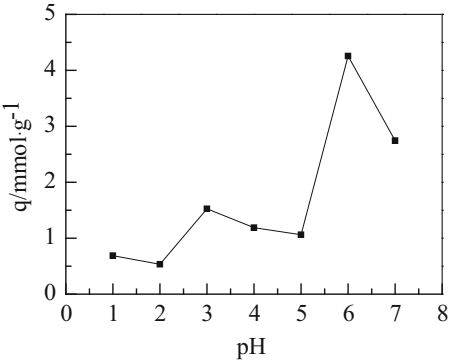

Fig. 6 Effect of pH on the adsorption of AO-PNS-*g*-PAN for Hg(II)

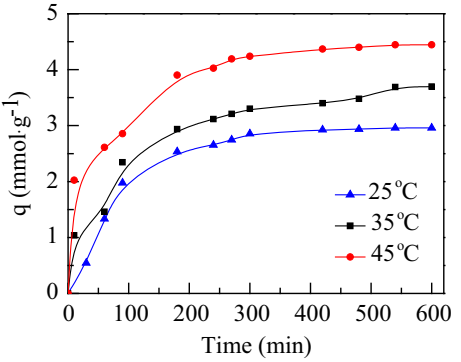

Fig. 7 Adsorption kinetics of AO-PNS-*g*-PAN for Hg(II)

consisted of two stages. The first stage showed a rapid adsorption pattern due to the large number of active sites available on the surface of AO-PNS-*g*-PAN. The second stage exhibited a gradual tendency because the active sites were progressively occupied by the metal ions which brought about no great difference in the adsorption rate. To explore the controlling mechanism of Hg(II) adsorption onto AO-PNS-*g*-PAN, pseudo-first-order and pseudo-second-order models were employed to explain the experimental data, as shown in Eqs. (4) and (5):

$$\ln\frac{(q_e - q_t)}{q_e} = -k_1 t \tag{4}$$

$$\frac{t}{q_t} = \frac{1}{k_2 q_e^2} + \frac{t}{q_e} \tag{5}$$

where q_e is adsorption capacity at equilibrium (mmol g^{-1}), k_1 is the rate constant of pseudo-first-order (min^{-1}), q_t is adsorption capacity at any time (mmol g^{-1}), k_2 is the rate constant of pseudo-second-order (g $mmol^{-1}$ min^{-1}).

The relevant parameters of the fitting results of pseudo-first-order and pseudo-second-order are summarized in Table 1. By comparing the correlation coefficients R^2 values, we can conclude that the pseudo-second-order model is more suitable to explain the adsorption kinetic processes at three temperatures. Moreover, the theoretical adsorption capacity q_e(cal) calculated from pseudo-second-order model is more close to the experimental adsorption capacity q_e(exp), which also can

Table 1 Kinetics parameters for adsorption of Hg(II) by AO-PNS-*g*-PAN at different temperatures

T (°C)	q_e(exp) (mmol g^{-1})	Pseudo-first-order kinetics			Pseudo-second-order kinetics		
		K_1 (min^{-1})	q_e (cal) (mmol g^{-1})	R_1^2	K_2 (g $mmol^{-1}$ min^{-1})	q_e(cal) (mmol g^{-1})	R_2^2
25	2.96	0.0106	3.16	0.9806	0.0036	3.05	0.9924
35	3.70	0.0051	2.22	0.9390	0.0043	3.80	0.9996
45	4.45	0.0120	5.99	0.8434	0.0044	4.54	0.9995

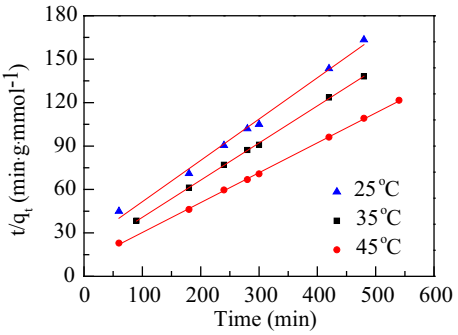

Fig. 8 Pseudo-second-order model of AO-PNS-*g*-PAN for Hg(II) at different temperatures

demonstrate the above conclusion. The corresponding fitting results of t/q_t versus t are shown in Fig. 8.

Adsorption isotherms

The adsorption isotherms of AO-PNS-*g*-PAN to Hg(II) at different temperatures were investigated and the results are depicted in Fig. 9. Similarly, there are two theories to describe the isothermal adsorption experimental data and they are Langmuir Eq. (6) and Freundlich isotherm model Eq. (7), respectively.

$$\frac{C_e}{q_e} = \frac{C_e}{q} + \frac{1}{qK_L} \tag{6}$$

$$\ln q_e = \ln K_F + \frac{\ln C_e}{n} \tag{7}$$

where q_e is the equilibrium adsorption capacity (mmol g^{-1}), C_e is the equilibrium concentration of metal ions (mmol mL^{-1}), q is the saturated adsorption capacity (mmol g^{-1}), K_L is an empirical parameter, K_F is the binding energy constant.

Langmuir model is applicable to a homogeneous surface and a monolayer adsorption process; while Freundlich model is an empirical equation describing a

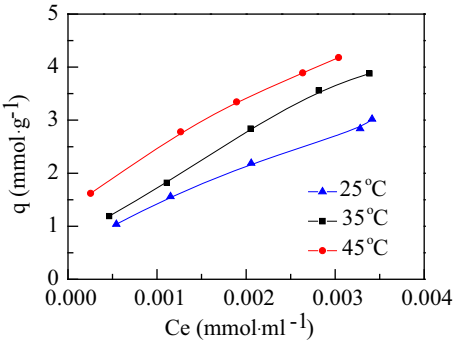

Fig. 9 Adsorption isotherms of AO-PNS-*g*-PAN for Hg(II) at different temperatures

Table 2 Langmuir and Freundlich parameters for adsorption of Hg(II) by AO-PNS-*g*-PAN at different temperatures

T (°C)	Langmuir parameters			Freundlich parameters		
	q_{the} (mmol g^{-1})	K_L	R_L^2	K_F	$1/n$	R_F^2
25	4.7998	452	0.9610	76	0.5728	0.9980
35	6.5963	400	0.9137	124	0.6102	0.9901
45	4.9702	1336	0.9559	36	0.3770	0.9915

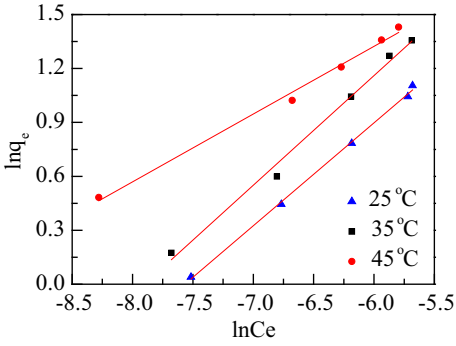

Fig. 10 Freundlich isotherm model of Hg(II) adsorbed on AO-PNS-*g*-PAN at different temperatures

heterogeneous system and a reversible adsorption process. The relevant coefficients of Langmuir and Freundlich model are summarized in Table 2. As illustrated in Table 2, the relatively high R_F^2 values suggested that the Freundlich isotherm model was more suitable to fit the experimental data. In other words, the adsorption process could be interpreted as a multilayer surface adsorption on the basis of the Freundlich model. Meanwhile, the fitting curve of Freundlich isotherm model is displayed in Fig. 10.

Conclusion

This study highlights the potential of agricultural residue containing amidoxime and hydroxyl groups as an efficient adsorbent to remove Hg(II). AO-PNS-*g*-PAN was synthesized by the processes of pretreatment of PNS, acylation with α-BrIBA, polymerization of AN and modification with $NH_2OH{\cdot}HCl$. The adsorption process depended on solution pH, contact time and initial metal ions concentration. The adsorption kinetics data followed the pseudo-second-order model and isotherm data could be described by the Freundlich isotherm model. PNS functionalized by amidoxime groups exhibited a greater capacity than crude PNS for Hg(II). PNS could be selected as a promising material to prepare the efficient adsorbent through introducing other functional groups.

Acknowledgments The finance was supported by the National Natural Science Foundation of China (Nos. 21404051 and 21404052), the Natural Science Foundation of Shandong Province (Nos. ZR2014BQ016 and BS2014CL040), the Talent Introduction Special Funds of Ludong University (Nos. 2014012 and 2014017), the Natural Science Foundation for Distinguished Young Scholars of Shandong province (No. JQ201203).

References

1. Demirbas A (2008) Heavy metal adsorption onto agro-based waste materials: a review. J Hazard Mater 157:220–229
2. Wan WS, Ngah MA, Hanafiah KM (2008) Removal of heavy metal ions from wastewater by chemically modified plant wastes as adsorbents: a review. Bioresour Technol 99:3935–3948
3. Aydin H, Bulut Y, Yerlikaya CJ (2008) Removal of copper (II) from aqueous solution by adsorption onto low-cost adsorbents. J Environ Manag 87:37–45
4. Kumar U, Bandyopadhyay M (2006) Sorption of cadmium from aqueous solution using pretreated rice husk. Bioresour Technol 97:104–109
5. Babarinde NAA, Oyebamiji Babalola J, Adebowale Sanni R (2006) Biosorption of lead ions from aqueous solution by maize leaf. J Phys Sci 1:23–26
6. Quek SY, Wase DAJ, Forster CF (1998) The use of sago waste for the sorption of lead and copper. Water SA 24:251–256
7. Zhang BW, Fischer K, Bieniek D, Kettrup A (1994) Synthesis of carboxyl group containing hydrazine-modified polyacrylonitrile fibres and application for the removal of heavy metals. React Polym 24:49–58
8. Deng SB, Bai RB, Chen JP (2003) Behaviors and mechanisms of copper adsorption on hydrolyzed polyacrylonitrile fibers. J Colloid Interface Sci 260:265–272
9. Niu YH, Qu RJ, Sun CM, Wang CH, Chen H, Ji CN (2013) Adsorption of Pb(II) from aqueous solution by silica-gel supported hyperbranched polyamidoamine dendrimers. J Hazard Mater 244–245:276–286
10. Vijayalakshmi A, Arockiasamy DL, Nagendran A, Mohan D (2008) Separation of proteins and toxic heavy metal ions from aqueous solution by CA/PC blend ultrafiltration membranes. Sep Purif Technol 62:32–38
11. Hawker CJ, Bosman AW, Harth E (2001) New polymer synthesis by nitroxide mediated living radical polymerizations. Chem Rev 101:3661–3688
12. Moad G, Rizzardo E, Thang SH (2008) Radical addition-fragmentation chemistry in polymer synthesis. Polymer 49:1079–1131
13. Barner-Kowollik C, Perrier S (2008) The future of reversible addition fragmentation chain transfer polymerization. J Polym Sci Part A: Polym Chem 46:5715–5723
14. Matyjaszewski K, Jiang X (2001) Atom transfer radical polymerization. Chem Rev 101:2921–2990
15. Nguyen NH, Percec V (2010) Dramatic acceleration of SET-LRP of methyl acrylate during catalysis with activated Cu(0) wire. J Polym Sci Part A: Polym Chem 48:5109–5119
16. Percec V, Guliashvili T, Ladislaw JS, Wistrand A, Stjerndahl A, Sienkowska MJ, Monteiro MJ, Sahoo S (2006) Ultrafast synthesis of ultrahigh molar mass polymers by metal-catalyzed living radical polymerization of acrylates, methacrylates, and vinyl chloride mediated by SET at 25 °C. J Am Chem Soc 128:14156–14165
17. Nguyen NH, Levere ME, Percec V (2012) TREN versus Me_6-TREN as ligands in SET-LRP of methyl acrylate. J Polym Sci Part A: Polym Chem 50:35–46
18. Nguyen NH, Percec V (2011) SET-LRP of methyl acrylate catalyzed with activated Cu(0) wire in methanol in the presence of air. J Polym Sci Part A: Polym Chem 49:4756–4765
19. Zhai SJ, Wang B, Feng C, Li YJ, Yang D, Hu JH, Lu G, Huang XY (2010) Thermoresponsive PPEGMEA-*g*-PPEGEEMA well-defined double hydrophilic graft copolymer synthesized by successive SET-LRP and ATRP. J Polym Sci Part A: Polym Chem 48:647–655
20. Johnson PD, Watson MA, Brown J, Jefcoat IA (2002) Peanut hull pellets as a single use sorbent for the capture of Cu(II) from wastewater. Waste Manag 22:471–480
21. Edlund U, Albertsson AC (2012) SET-LRP goes "green": Various hemicellulose initiating systems under non-inert conditions. J Polym Sci Part A: Polym Chem 50:2650–2658

22. Voepel J, Edlund U, Albertsson AC, Percec V (2011) Hemicellulose-based multifunctional macroinitiator for single-electron-transfer mediated living radical polymerization. Biomacromolecules 12:253–259
23. de Santa Mariaa LC, Amorimb MCV, Aguiara MRMP, Guimaraesa PIC, Aguiarb MAS, de Costaa AP, Rezende PR, de Carvalho MS, Barbosa FG, Andrade JM, Ribeiro RCC (2001) React. Chemical modification of cross-linked resin based on acrylonitrile for anchoring metal ions. Funct Polym 49:133–143
24. Zhao T, Zhang LF, Zhang ZB, Zhou NC, Cheng ZP, Zhu XL (2011) A novel approach to modify poly(vinylidene fluoride) via iron-mediated atom transfer radical polymerization using activators generated by electron transfer. J Polym Sci Part A Polym Chem 49:2315–2324
25. Anirudhan TS, Divya LPS (2009) Kinetic and equilibrium characterization of uranium(VI) adsorption onto carboxylate-functionalized poly(hydroxyethylmethacrylate)-grafted lignocellulosics. J Environ Manag 90:549–560
26. Liu YH, Zhou WQ, Bai LB, Zhao N, Liu YW (2006) Graft copolymerization of styrene onto casein initiated by potassium diperiodatonickelate (IV) in alkaline medium. J Appl Polym Sci 100:4247–4251
27. Bai LB, Zhao K, Wu YG, Li WL, Wang SJ, Wang HJ, Ba XW, Zhao HC (2014) A new method for synthesizing hyperbranched polymers with reductive groups using redox/RAFT/SCVP. Chin J Polym Sci 32:385–394
28. Xiong L, Chen C, Chen Q, Ni JR (2011) Adsorption of Pb(II) and Cd(II) from aqueous solutions using titanate nanotubes prepared via hydrothermal method. J Hazard Mater 189:741–748
29. Liu CK, Bai RB, Ly QS (2008) Selective removal of copper and lead ions by diethylenetriamine-functionalized adsorbent: behaviors and mechanisms. Water Res 42:1511–1522
30. Monier M, Abdel-Latif DA (2012) Preparation of cross-linked magnetic chitosan-phenylthiourea resin for adsorption of Hg(II), Cd(II) and Zn(II) ions from aqueous solutions. J Hazard Mater 209–210:240–249
31. Niu YZ, Qu RJ, Chen H, Mu L, Liu XG, Wang T, Zhang Y, Sun CM (2014) Synthesis of silica gel supported salicylaldehyde modified PAMAM dendrimers for the effective removal of Hg(II) from aqueous solution. J Hazard Mater 278:267–278